Comparative characterisation and phytotoxicity assessment of biochar and hydrochar derived from municipal wastewater microalgae biomass

Bioresource Technology 386 (2023) 129567

Contents lists available at ScienceDirect

Bioresource Technology

journal homepage: www.elsevier.com/locate/biortech

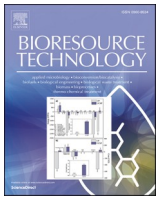

Comparative characterisation and phytotoxicity assessment of biochar and hydrochar derived from municipal wastewater microalgae biomass

Jiacheng Sun [a,*], Veronica Benavente [b,c], Stina Jansson [b], Ondřej Mašek [a]

[a] UK Biochar Research Centre, School of Geosciences, University of Edinburgh, Crew Building, Alexander Crum Brown Road, Edinburgh EH9 3FF, UK
[b] Department of Chemistry, Umeå University, SE-90187 Umeå, Sweden
[c] RISE Processum AB, SE-89122 Örnsköldsvik, Sweden

HIGHLIGHTS

- Municipal wastewater derived microalgae are used to produce biochar and hydrochar.
- Microalgae biochar promotes the germination and seedling growth.
- Microalgae hydrochar can inhibit the germination due to the organic acids.
- Post-pyrolysis and organic solvent washing are proved to be effective methods mitigating phytotoxicity of hydrochar.

GRAPHICAL ABSTRACT

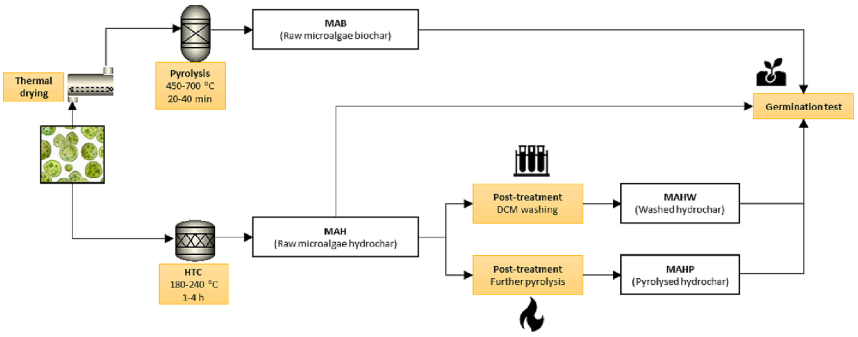

ABSTRACT

Microalgae, originating from a tertiary treatment of municipal wastewater, is considered a sustainable feedstock for producing biochar and hydrochar, offering great potential for agricultural use due to nutrient content and carbon storage ability. However, there are risks related to contamination and these need to be carefully assessed to ensure safe use of material from wastewater microalgae. Therefore, this study compared the properties and phototoxicity of biochar and hydrochar produced via pyrolysis and hydrothermal carbonisation (HTC) of microalgae under different temperatures and residence times. While biochar promoted germination and seedling growth by up to 11.0% and 70.0%, respectively, raw hydrochar showed strong phytotoxicity, due to the high content of volatile matter. Two post-treatments, dichloromethane (DCM) washing and further pyrolysis, proved to be effective methods for mitigating phytotoxicity of hydrochar. Additionally, biochar had 35.8–38.6% fixed carbon, resulting in higher carbon sequestration potential compared to hydrochar.

1. Introduction

In recent years, microalgae have received much attention regarding their potential role in wastewater treatment, based on their ability to use inorganic nitrogen (N) and phosphorus (P) for their growth, and thereby reduce the concentration of these compounds in the wastewater (Mohsenpour et al., 2021). As part of wastewater treatment processing, microalgae cultivation provides a tertiary biotreatment strategy coupled with production of potentially valuable biomass (Abdel-Raouf et al., 2012). Unlike lignocellulosic biomass which mainly consists of cellulose, hemicellulose, and lignin, microalgae biomass contains lipids, carbohydrates, and proteins, which makes it a potential renewable N source for alternative fertilisers, or fertiliser additives (Sun et al., 2021).

Remediation of nutrients using conventional treatment technologies

* Corresponding author.
E-mail address: jiacheng.sun@hotmail.com (J. Sun).

https://doi.org/10.1016/j.biortech.2023.129567
Received 16 June 2023; Received in revised form 20 July 2023; Accepted 25 July 2023
Available online 26 July 2023

is costly (Shyam et al., 2022); therefore, exploring an organic and cost-effective method to recover wastewater nutrients using microalgae biomass would offer substantial benefits. The primary advantage of microalgae-based treatment methods is that they do not require additional energy input to effectively recover nutrients, in contrast to conventional methods like microfiltration and sludge activation, which need large energy inputs (Li et al., 2022). Dedicated cultivation of microalgae requires significant nutrient inputs, and therefore growing microalgae in wastewater presents a win–win scenario where the high nutrient demand of microalgae cultivation can be largely met by utilising nutrient-rich wastewater from industrial and municipal sources while simultaneously cleaning it.

Algae derived biochar can be produced using thermochemical conversion processes, such as pyrolysis and hydrothermal carbonisation (HTC), which not only have good energy efficiency but also produce nutrient-rich char products that can be used as fertiliser additives. Pyrolysis is a thermal decomposition process transforming organic material into solid, liquid, and gaseous products under an oxygen-limited atmosphere at temperatures ranging from 350 °C to 1000 °C (European Biochar Foundation (EBC), 2016; IBI, 2015). HTC on the other hand, sometimes referred to as wet pyrolysis, can be used to process a wide range of moisture-rich feedstocks such as algae biomass, municipal wastes, and wet lignocellulosic biomass (Bevan et al., 2020). This feature of HTC makes it an effective thermochemical process without the need for an energy-intensive and costly drying of the feedstock prior to carbonisation.

Under HTC conditions, various reactions occur including dehydration, decarboxylation, decarbonylation, polymerisation, which result in the formation of carbon-rich solid products and the release of gaseous and liquid byproducts. The composition of hydrochar, the primary product of HTC, differs significantly from that of biochar in terms of carbon and hydrogen percentages, depending on the type of feedstock used. This is because HTC undergoes less aromatisation and dehydration (Mumme et al., 2018), while polymerisation and condensation reactions in the liquid phase lead to the formation of carbon structures (secondary char) on the surface of the primary char (Lucian et al., 2018). The formation of organic acids also reduces the pH value of hydrochar (Mumme et al., 2018). Biochar has higher ash content because most minerals are retained in the solid during pyrolysis, which results in a higher pH value (Mumme et al., 2018). Compared to biochar, the higher degree of oxygen-containing functionalities on the hydrochar surface explains its high affinity for water; hence this property would result in a better water retention capacity of the soil (Kambo and Dutta, 2015). In addition, the cost of producing biochar from high-moisture biomass is influenced by the energy-intensive drying process required, which could also cause additional environmental concerns. In contrast, HTC can accommodate high-moisture feedstocks without the need for a separate drying step, making HTC an attractive option for this type of materials.

Although pyrolysis requires more energy compared to HTC, it has the advantage of generating syngas than can serve as an energy source to supply heat for the pyrolysis furnace, making pyrolysis a more practical option. A previous research conducted by Cong et al. demonstrated that pyrolysis of corn stover at temperatures ranging from 550 to 650 °C can produce pyrolytic gas with an HHV of approximately 20 MJ/Nm^3, providing a valuable gaseous fuel to fully meet the heating requirements of the pyrolysis system (Cong et al., 2018). Additionally, when considering carbon sequestration potential, biochar exhibits superior carbon stability compared to hydrochar, making it a more favourable product (Kambo and Dutta, 2015). In recent years, there has been a growing interest in studying mineral-rich biochar to enhance carbon sequestration and improve properties relevant to environmental applications. For example, Mašek et al. (2019) indicated that potassium (K) doping increases biochar carbon sequestration by 45%, which facilitates reaching a carbon sequestration potential over 2.6 Gt CO_2-C(eq) yr^{-1}. As for biochar production, higher mineral content feedstocks (both inherent and added ash-forming elements) usually display higher biochar yields (Buss et al., 2021). The catalytic effect of alkaline metals on biochar formation and the low propensity of ash-forming elements to enter the vapour phase during pyrolysis are two important factors explaining the higher solid fraction yield (Buss et al., 2021, 2019; Mašek et al., 2019). Furthermore, mineral species in biomass also affect biochar co-products. According to research conducted by Wurzer and Mašek (2021), biochar production using Fe-doped feedstock resulted in a significantly higher pyrolysis gas yield (approximately 50%) and associated energy content in the gaseous co-products (around 40% HHV). This, in turn, helped to reduce the cost of biochar production when the gaseous products were utilised as energy input. In addition, it was observed that Fe doping enhanced the removal capacity of biochar adsorbents for organic contaminants like caffeine and fluconazole by up to four times (Wurzer and Mašek, 2021).

Some studies have indicated that microalgae hydrochar can also serve as a plant cultivation media. According to a study conducted by Chu et al. (2020), the application of *Chlorella vulgaris* hydrochar to rice paddy soil resulted in a 26.7% increase in rice yield and a boost in the production of soluble sugars within the rice grains. A similar study by de Jager and Giani (2021) concluded that application of plant- and animal-based digestate-residue derived hydrochar in podzol soil can increase seed germination rate from about 54 to 80%. However, applying microalgae hydrochar in the soil might concomitantly increase the NH_3 volatilisation and N_2O emissions from the soil. Zhou et al. (2018) found that even with the optimal application rate of hydrochar in soil, the N_2O emissions still amounted to 6.0–32.3%. Thus, finding a cost-effective and environmentaly-friendly post-treatment that imitigates the increase potential for NH_3 and N_2O emissions from raw hydrochar application is critical.

This study is a continuation of previous work conducted by Benavente et al. (2022), in which microalgae biomass was converted into hydrochar and examined using e.g. Py-GC/MS to identify potentially phytotoxic components. The previous work found the formation of secondary char caused the phytotoxicity of hydrochar, and lipid extraction of biomass can reduce the impact. Subsequently, this study aims to further examine the toxicological impact of microalgae-derived biochar and hydrochar, and specifically assess its effect on seed germination and seedling growth. So far, this is the first study to quantitatively determine this effect on soil amendment performance of microalgae biochar and hydrochar. The study provides information that can be used to conduct an environmental risk assessment of microalgae biochar and hydrochar. This supports the safe utilisation of biochar and hydrochar in soil applications.

2. Materials and methods

2.1. Microalgae biomass

This study involved culturing microalgae in two raceway ponds at the Umeå Energi combined heat and power plant in Sweden, using untreated municipal wastewater and flue gases containing 10% CO_2 (v/v). Microalgae biomass was harvested from the ponds and characterised to determine its carbohydrate, protein, and ash contents, with analysis showing that it had 26.3 ± 8.5% carbohydrates, 26.9 ± 3.3% proteins, and 16.4 ± 4.6% ash, which were described in Benavente et al. (2022).

2.2. Pyrolysis

The microalgae paste, subjected to a 105 °C oven drying process, underwent homogenisation, crushing, and grinding using a mortar and pestle. Subsequently, the resulting solids were sieved to achieve a particle size range of 0.25–0.85 mm. Approximately 70% by weight of the initial dry microalgae paste successfully attained the desired target size. A pyrolysis system at the UK Biochar Research Centre (UKBRC), University of Edinburgh, referred to as Stage I, was used, described in more detail by Mašek et al. (2018). The set-up was a 50 mm diameter vertical

quartz tube batch reactor, heated by an infra-red gold image furnace (P610C; ULVACRIKO, Yokohama, Japan). The batch reactor was connected to a condensation system in which different fractions of condensable volatile vapours were collected in a heat trap (120 °C), an ambient trap (25 °C), and two cold traps (both approximately 0–5 °C), while non-condensable gases were collected in gas bags for further analysis. A thermocouple was set inside the batch reactor, positioned approximately 10 mm from the inner surface of the quartz tube. Prior to the experiment, a nitrogen flow of 40 L/min was supplied to achieve an inert environment during pyrolysis, and to carry volatile vapours and gaseous products into the condensation system. Nitrogen flow monitoring and gas analysis was conducted using a Volumetric Flow Meter (TG5; Ritter, Bochum, Germany) and a Multi-gas Analyser (Rapidox 5100; Cambridge Sensotec, UK).

Approximately 20 g of dried and sieved microalgae was placed at the centre of the heating reactor. The reactor was heated to 450, 550, and 700 °C, respectively, at a heating rate of 25 °C/min. Two different residence times were examined, i.e., 20 and 40 min, respectively. To calculate the yields of both solid and liquid, this study used the difference in weight of each apparatus before and after conducting the experiments. The biochar samples were labelled MAB-T-t, where T refers to pyrolysis temperature and t refers to residence time.

2.3. Hydrothermal carbonisation (HTC)

HTC processing of microalgae was carried out as described in Benavente et al. (2022). In brief, 650 g of microalgae paste with 15% solid content was processed in a stainless-steel reactor equipped with water-cooling (Amar Equipments Pvt. Ltd.). After the set residence time, the reactor reached ambient temperature aided by the internal water-cooling system and was depressurized by discharging the gaseous products to the fume extractor. To separate the products, the resulting slurry was centrifuged at 4700 rpm for 20 min. The solid fraction, i.e., the hydrochar, was washed twice with 500 mL ultrapure water, and then dried in an oven at 65 °C.

In this study, raw hydrochars were produced at temperatures of 180, 210, 240 °C, and residence times of 1, 2, and 4 h, resulting in a total of 9 hydrochars. The obtained raw hydrochar samples were labelled MAH-T-t, where 'T' refers to HTC temperature and 't' refers to residence time.

2.4. Proximate and elemental analysis

Proximate analysis is a widely used method for determining moisture, volatile matter (VM), fixed carbon (FC), and ash content of biochar, as well as hydrochar. Thermogravimetric analysis with differential scanning calorimetry was conducted using a TGA with autosampler (TGA/DSC-1; Mettler-Toledo, Leicester, UK) at the UKBRC. Around 10 mg of biochar/hydrochar samples were initially placed in alumina crucibles, followed by the moisture determination according to the percentage mass loss on heating to 110 °C under nitrogen flow for 10 min. This step aimed to thoroughly dry the samples and eliminate moisture absorbed by feedstock and char samples during storage and transportation. Then the samples were further heated to 900 °C at a heating rate of 25 °C/min and kept at that temperature for 10 min to determine volatile matter content. After this, the purge gas was switched from nitrogen to air and the sample was combusted for a period of 30 min to determine ash content. Fixed carbon content was calculated on a weight percent basis by subtracting moisture, volatile matter, and ash content from the initial mass of the sample. Each analysis was performed in triplicate.

Samples were ground to a fine powder and dried at 105 °C before elemental analysis. Approximately 1.5 mg of the dried sample was weighed out with an accuracy of 0.001 mg in a Sartorius SC2 microbalance, double wrapped into tin capsules and stored in a desiccator. The samples then were burned at a high temperature followed by separating and measuring the gases produced, which allows the amounts of carbon, nitrogen, hydrogen and sulphur to be determined. Concentrations of oxygen were determined by high-temperature pyrolysis. The CHNS/O analysis was conducted using an Organic Elemental Analyser (FlashSmart 2000; Thermo Fisher Scientific, Waltham, MA, USA). Each analysis was performed in triplicate.

2.5. ICP-MS analysis

The fine-ground (0.06–0.5 mm) biochar and hydrochar samples were digested with 5% v/v nitric acid solution using the Modified Dry Ash method, according to Benavente et al. (2022). The obtained solutions were then diluted to keep dissolved solid contents lower than 0.2%. Controlled blanks were also included, intended to screen any contamination in the digestion stages. The phosphorus (P), potassium (K), calcium (Ca), magnesium (Mg), sodium (Na), manganese (Mn), and boron (B) contents were determined using an Agilent 7500ce inductively coupled plasma mass spectrometry (ICP–MS) (Santa Clara, CA, USA) at the School of Chemistry, University of Edinburgh, with rf forward power 1,540 W and reflected power 1 W, and Ar gas flows of 0.81 and 0.19 L min $-$ 1 for carrier and makeup flows, respectively. A semi-quantitative scan was conducted to analyse the elements which were not presented in calibration solutions. All analyses were performed in triplicate.

2.6. Electric conductivity (EC) and pH

For pH measurement, 1 g of ball-milled biochar or hydrochar was mixed with 20 mL of deionized and shaken for 1.5 h to ensure the equilibration between biochar or hydrochar surfaces and solution according to Benavente et al. (2022) which is recommended by the International Biochar Initiative (IBI, 2015). A Mettler Toledo FE 30 was used for pH determination. The EC of biochar or hydrochar was then determined by a HM digital EC probe (model COM-100).

2.7. Germination test and seedling growth

A 1% application rate (approximately corresponding to 22.5 t/ha) in pure sand was used. To reach the 1% application rate 29.7 g sand and 0.3 g biochar or hydrochar were mixed, and 6.6 g of DI water was also added to the mixture to reach 80% of its water holding capacity (WHC). A filter paper with 0.9 g DI water was used at the bottom of the petri dish, which was equivalent to 80% of the WHC.

The mixture was weighed in a plastic bag, with approximately 36.6 g mixture added to each petri dish. Then, 10 seeds of watercress (*Nasturtium officinale*) were spread randomly on the top of the mixture. The germination tests were replicated three times for each sample. The petri dishes were sealed with parafilm to prevent drying. In this early stage, the seeds require only small amounts of gases, and mainly oxygen, all of which should be sufficient also when sealed. The sealed petri dishes were stored in a temperature-controlled room at around 25 °C. Each petri dish was placed in an angle of 50° for seven days to germinate. The reason for using a 50-degree angle is to ensure that the roots grow downwards in a consistent manner, allowing for easier comparison of root growth. Seeds are considered germinated if the root or shoot is longer than half the length of the seed. Root and shoot length were determined by image analysis using software ImageJ version 1.50i. The whole experiment was kept as clean as possible, ideally sterilising the equipment as these were perfect conditions for fungal growth in the petri dishes.

2.8. Post-treatment for hydrochar

The extractable portion of raw hydrochar, which comprised fatty acids and secondary char, was separated from the insoluble hydrochar structure assigned to the primary char using dichloromethane (DCM) as described in Benavente et al. (2022). An Erlenmeyer flask was filled with

20 mL DCM per gram of dry hydrochar and vortexed for 30 min at room temperature. Vacuum filtering through a Whatman grade GF/C glass microfiber filter (1.2 m) was conducted to separate the solid, which was then washed with 8 mL of fresh DCM per gram of solid. The as-obtained solids were labelled as MAHW-T-t, where T refers to HTC temperature and t refers to residence time. The DCM washing was conducted at Umeå University, Sweden.

Another group of raw hydrochar was further pyrolysed using the Stage I unit mentioned in Section 2.1. Specifically, all hydrochar samples were pyrolysed in the batch reactor and heated up to 550 °C at a rate of 25 °C/min and maintained isothermally for 40 min. Afterward, the reactor was cooled to room temperature at a rate of 25 °C/min. The as-obtained pyrolysed hydrochar were labelled as MAHP-T-t, where T refers to HTC temperature and t refers to residence time. The DCM washed hydrochar and pyrolysed hydrochar were kept in centrifuge tubes (Fisherbrand®) and stored at ambient temperature for further analyses.

2.9. Carbon sequestration potential

For both microalgae biochar and hydrochar, carbon sequestration potential (*CSP*) is an important parameter that can be calculated from the following equation:

$$CSP(\%) = \frac{Fixedcarbonincharproducts(\%)}{carboncontentinmicroalgaebiomass(\%)} \times 100\% \quad (1)$$

3. Results and discussion

3.1. Performance of pyrolysis and HTC

The effects of the highest temperature and residence time on biochar and hydrochar yields are shown in Fig. 1 and pyrolytic product yields are presented in (see supplementary material). It has been observed that the solid product yield declines significantly with a rise in temperature, which is consistent with the findings in the HTC and pyrolysis literature. With an increase in HTC temperature from 180 to 240 °C, the yields of hydrochar decreased from 54.9% to 38.7%, as shown in previous study (Benavente et al., 2022). For the biochar, the yields decreased from 36.9% to 32.2% with an increase in pyrolysis temperature from 450 °C to 700 °C. Microalgae pyrolysis involves dehydration (<200 °C),

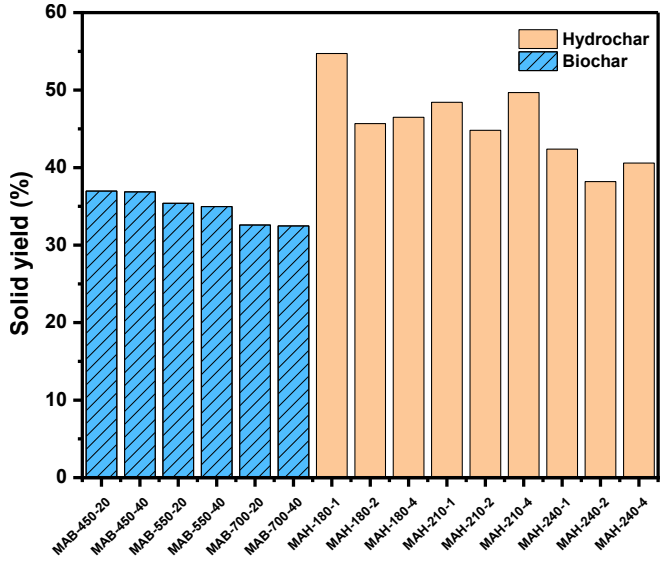

Fig. 1. Biochar and hydrochar yields from microalgae at different temperatures and residence times. Biochar samples were labelled MAB-T-t, where T refers to pyrolysis temperature and t refers to residence time. Similarly, hydrochar samples were labelled MAH-T-t.

devolatilisation of carbohydrates and proteins (200–500 °C), decomposition of lipids (350–550 °C), and decomposition of more heat-resistant components (550–800 °C), while pyrolysis of lignocellulosic biomass decompose hemicellulose, cellulose, and lignin at 220–315 °C, 314–400 °C, and 160–900 °C, respectively (Sun et al., 2021). On the other hand, microalgae HTC decomposes long-chain polymers into small molecules via hydrolysis and depolymerisation at < 190 °C, and then dehydration and decarboxylation occurs up to 260 °C (Castro et al., 2021); this is similar for HTC of lignocellulosic biomass (Khan et al., 2019). The described reaction mechanisms of microalgae and lignocellulosic pyrolysis and HTC can well explain the decreased solid yields with increased temperature. As a result, highly aromatic structures were expected in the high-temperature char products.

On the other hand, the longer residence time can enhance decomposition and aromatisation during thermal conversion, but the impact was not as significant as that of temperature. Nevertheless, the hydrochar yields decreased significantly over the residence time range of 1 h to 2 h and slightly increased from 2 h to 4 h. This result could be explained by increased polymerisation and formation of secondary char on the surface of primary hydrochar during 2–4 h, as described in Benavente et al. (2022). In contrast to lignocellulosic HTC (Zhang et al., 2015), the microalgae HTC examined in this study exhibited higher yields as residence time increased. A possible explanation might be that protein- and lipid-based microalgae feedstock would generate more liquid products than lignocellulosic biomass during HTC. The moderate-temperature environment can promote polymerisation and condensation, which results in higher solid yields with longer residence time. Further investigation of the secondary char formed on microalgae hydrochar is needed for potential applications such nutrient recovery and electrode material (Sun et al., 2021).

This study highlights how the proximate composition and species of the algae feedstock can significantly affect the performance of pyrolysis and HTC. Due to the unique growing environment (wastewater), the microalgae mixture collected as part of this study exhibited a relatively high ash content (15.8 wt%) when compared to common microalgae species such as *Nannochloropsis*, *Spirulina*, and *Chlorella vulgaris*. As a consequence, high yields of pyrolytic biochar were generated in this study. The high ash content of the microalgae mixture used here, and of several common macroalgae species, might make them good feedstocks for biochar production and hence prospective high-nutrient soil improvers. The nutrient content of microalgae biochar and hydrochar are discussed in Section 3.2. Hydrochars, on the other hand, had greater solid yields than biochars due to the lower heating temperature. In contrast to pyrolysis, the hydrochar yield differential between microalgae and macroalgae was not significant. Hence, it is critical to select the appropriate algae species for each specific application. In short, the high ash content and low volatile matter content of the microalgae mixture used in this study is indicative of char products which are promising as soil amendments.

3.2. Material characteristics

The ultimate analysis data is presented on a dry ash-free basis due to the large difference between the ash contents of biochar and hydrochar (Table 1). As expected, with increasing temperature the carbon content in biochar and hydrochar increased considerably, indicating progress of carbonisation as a result of heating. The N content of produced biochar (9.3–11.2 daf%) and hydrochar (5.7–6.5 daf%) were significantly higher compared to other lignocellulose derived biochars and hydrochars, due to the high protein content in the microalgae biomass. Nitrogen-enriched biochar possesses several promising advantages such as high gas adsorption ability (Zhang et al., 2022) and unique soil amendment. For example, a nitrogen-enriched biochar modified by ZIF-8 grafting and annealing showed 260% CO_2 adsorption ability after modification by enhancing the van der Waals interaction between the biochar and CO_2 molecules (Zhang et al., 2022). Another research studied a nitrogen-

Table 1
Influence of temperature and residence time on the composition of biochar and hydrochar produced from microalgae biomass, (results are reported as mean ± standard deviation, number of replicates = 3).

Sample name	Proximate analysis (wt%)			Ultimate analysis (dry ash-free basis) (daf%)				
	VM	FC	Ash	C	H	N	S	O
MAB-450–20	22.50 ± 0.20	35.81 ± 0.26	41.69 ± 0.47	70.88 ± 0.09	6.81 ± 0.13	11.23 ± 0.10	0.43 ± 0.03	10.65 ± 0.05
MAB-450–40	24.63 ± 1.63	34.10 ± 2.06	41.26 ± 0.43	70.63 ± 1.10	3.90 ± 0.03	10.32 ± 0.07	0.43 ± 0.03	14.73 ± 0.04
MAB-550–20	20.10 ± 0.55	36.90 ± 0.31	43.00 ± 0.86	76.12 ± 2.15	3.39 ± 0.02	11.14 ± 0.23	0.30 ± 0.04	9.05 ± 0.75
MAB-550–40	18.89 ± 0.54	37.24 ± 0.07	43.87 ± 0.48	74.68 ± 0.61	3.37 ± 0.04	10.69 ± 0.09	0.36 ± 0.00	10.90 ± 0.76
MAB-700–20	16.31 ± 0.07	38.36 ± 1.42	45.32 ± 1.49	79.77 ± 0.45	2.40 ± 0.03	9.47 ± 0.05	0.37 ± 0.06	7.99 ± 0.22
MAB-700–40	15.00 ± 0.67	38.68 ± 1.23	46.32 ± 0.56	80.64 ± 0.33	2.29 ± 0.01	9.31 ± 0.03	0.52 ± 0.03	7.23 ± 0.05
MAH-180–1	57.34 ± 0.34	17.05 ± 0.22	25.61 ± 0.57	63.95 ± 0.03	7.71 ± 0.88	6.50 ± 0.23	0.19 ± 0.07	21.65 ± 1.09
MAH-180–2	58.17 ± 0.15	15.61 ± 0.23	26.22 ± 0.38	64.86 ± 0.86	7.16 ± 1.20	6.02 ± 0.55	0.01 ± 0.00	21.94 ± 0.25
MAH-180–4	56.56 ± 1.22	16.20 ± 1.01	27.24 ± 0.21	65.60 ± 0.34	8.44 ± 0.23	5.90 ± 0.04	0.14 ± 0.01	19.93 ± 0.62
MAH-210–1	55.47 ± 0.98	17.09 ± 0.44	27.44 ± 0.53	67.75 ± 0.65	7.03 ± 0.43	5.86 ± 0.39	0.28 ± 0.02	19.08 ± 1.55
MAH-210–2	54.06 ± 0.11	17.24 ± 0.10	28.70 ± 0.01	69.16 ± 1.23	7.21 ± 0.98	6.01 ± 0.02	0.19 ± 0.03	17.44 ± 0.98
MAH-210–4	54.26 ± 0.13	16.68 ± 0.22	29.06 ± 0.35	68.82 ± 0.34	8.93 ± 1.01	6.42 ± 0.56	0.01 ± 0.00	15.81 ± 0.11
MAH-240–1	52.96 ± 0.98	17.50 ± 1.11	29.54 ± 0.13	71.32 ± 0.54	8.68 ± 0.13	6.49 ± 0.11	0.28 ± 0.04	13.23 ± 0.28
MAH-240–2	53.33 ± 1.03	17.31 ± 0.55	29.35 ± 0.48	72.84 ± 0.86	7.88 ± 0.96	6.43 ± 0.14	0.14 ± 0.01	12.71 ± 0.03
MAH-240–4	54.26 ± 0.99	16.86 ± 0.23	29.06 ± 0.76	73.49 ± 0.87	8.87 ± 0.11	5.72 ± 0.95	0.01 ± 0.00	11.90 ± 0.23

enriched biochar that has potential as a fertiliser (Yin et al., 2021). This biochar has ability to convert Fe^{3+} and Fe^{2+} in soil, leading to lower emission of CH_4 and CO_2, which can help improve sustainable food production and minimise negative environmental impacts. In this work, although hydrochar had a lower content of N compared to biochar, when the char yields were considered, the fraction of N contained in the raw microalgae material that was retained in biochar and hydrochar was comparable, i.e. 23.2–38.5% in hydrochar and 23.1–34.6% in biochar, with the rest released in the liquid and gaseous products. The results indicated that N-containing organic components had great thermal stability even at the highest temperature (i.e. 700 °C) during pyrolysis. This high N thermal stability can be possibly used as an effective strategy for gas adsorption in the future when algae biochar/hydrochar production is combined with high-temperature activation (Yin et al., 2021). This is due to the presence of increased active sites, such as pyrrolic N and graphitic N, which can enhance the binding between gas molecule and algae biomaterials which has potential implications for the development of more efficient and sustainable methods for gas capture and utilisation, especially for CO_2 (Yin et al., 2021).

Results in Fig. 2 showed that the hydrogen to carbon molar ratio (H/C) and oxygen to carbon molar ratio (O/C) for all biochar and hydrochar samples were in the range of 0.03–1.56 and 0.07–0.37, respectively. Because most of the VM were reduced during thermal conversion, the H/C and O/C ratios of all char products were lower than those of the

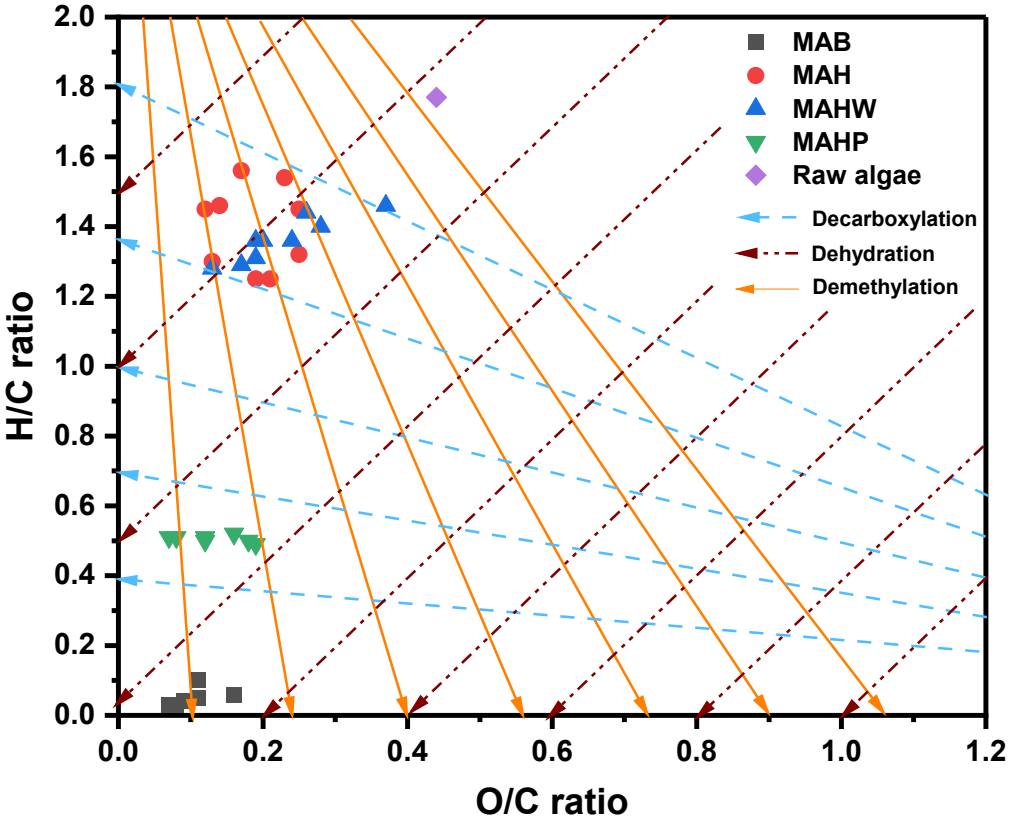

Fig. 2. Van-Krevelen-diagram showing raw microalgae, microalgae biochar (MAB), microalgae hydrochar (MAH), microalgae hydrochar with DCM washed (MAHW), and microalgae hydrochar with further pyrolysis (MAHP).

precursor microalgae. As the temperature increased, both ratios decreased, providing further support for increased carbonisation. The Van Krevelen diagram representing the examined biochars and hydrochars (Fig. 2) showed that the H/C ratio of MAB was significantly lower than 0.7, which met the International Biochar Initiative (IBI) standard as a material with great fused aromatic ring structures suitable for carbon sequestration (IBI, 2015). The O/C ratio of MAB was also dramatically lower than the European Biochar Certificate (EBC) standard limit (0.4), which indicated great stability of the biochar (European Biochar Foundation (EBC), 2016). The H/C ratio decreased in the order MAHP ≈ MAH > MAHP > MAB, implying that 1) MAB had the highest stability; 2) post-pyrolysis can be a possible and effective strategy (H/C modified from 1.3 to 0.5 approximately) to enhance the stability of microalgae hydrochar. 3) DCM washing had a mild impact on improving the stability of microalgae hydrochar. Generally, complex reactions existed in the pyrolysis and HTC, including decarboxylation, dehydration, demethylation, etc. (Bahcivanji et al., 2020). According to Fig. 2, it can be assumed that decarboxylation and dehydration reactions dominated during pyrolysis and HTC, and that a higher extent of dehydration occurred in pyrolysis due to the high reaction temperature. The dehydration reactions mainly came from the incomplete degradation of carbohydrates and proteins below 350 °C and the subsequent high temperature depolymerisation above 350 °C (Fu et al., 2019). Unlike pyrolysis, HTC provided an aqueous atmosphere to transform lipids into secondary char observed by Benavente et al. (2022), which can be responsible for part of the hydrolysis pathway. A noteworthy finding was the desirable H/C ratio of MAB (0.03–0.10) with high degree of conversion, which could indicate its suitability as carbon sequestration agent and as energy-intensive solid fuel. The two post-treatments – further pyrolysis and DCM washing – will be discussed in Section 3.4 and 3.5.

The results of the proximate analysis for biochar and hydrochar (Table 1) showed that with pyrolysis temperature increasing from 450 to 700 °C, the VM content of microalgae biochar decreased from 24.6 to 15.0 wt%. A similar effect was observed for the residence time, which reduced VM content for biochar produced in runs with higher residence time at peak temperature, as this allowed for a higher degree of conversion. For biochar produced at 450 °C on the other hand, the VM content increased with higher residence time. A potential explanation for this observation could be that the lipids that are more resistant to heat were not completely broken down during the 450 °C pyrolysis process, which caused them to remain in the biochar as VM components. Even with prolonged residence durations, these components did not decompose (Sun et al., 2021). On the other hand, the other components, such as indole (Gautam et al., 2017), aniline (Wang and Brown, 2013), and glucose (Ho et al., 2013), showed a continuous breakdown with increasing residence durations, resulting in a higher percentage of VM in the biochar produced at 450 °C pyrolysis with a 40-minute residence time, as indicated by the biochar yield. Compared to biochar, the VM content of all hydrochar was considerably higher, ranging between 52.9 and 58.1 wt%. Consequently, the FC content of the hydrochar was lower, suggesting a lower degree of carbonisation. Both biochars and hydrochars showed considerably higher content of ash compared to data for corresponding products from similar feedstocks in published literature (Ding et al., 2021; Gai et al., 2013; Lee et al., 2018; Michalak et al., 2019). The high ash contents were related to the origin of the microalgae polyculture, i.e. from a wastewater pond, which resulted in nutrient-rich chars. As a comparison, extensive literature has reported on the ash content of biochar derived from these single microalgal strains, namely, Scenedesmus (5.9 wt%) (Magida et al., 2021), Coelastrum (2.7 wt%) (Zheng et al., 2017), and Chlorella (2.1–6.0 wt%) (Binda et al., 2020), which were all significantly lower than the microalgae polyculture in this work (15.8 wt%). As a result, these high ash char products has a number of potential applications such as soil amendment, adsorption agent, and catalyst (Sun et al., 2021).

To gain further insights into the composition of mineral matter contained in the microalgae biochar and hydrochar, a detailed elemental analysis was conducted using inductively coupled plasma mass spectrometry (ICP-MS) (Fig. 3). A number of alkali and alkaline earth metals were present in the samples, which could explain the elevated pH of biochar (Table 2), while also increasing the conversion of organic O into inorganic O, e.g. newly formed carbonates (Bakshi et al., 2020). The hydrochar samples had relatively low trace element contents (about 50% lower) compared to biochar, but still notably higher than that of microalgae biochar produced by previous research (Michalak et al., 2019). Thus, the microalgae hydrochar produced in this study, with its potential ability to release nutrients and carbon sequestration, might also be an environmentally benign soil additive for plant growth, especially Fe, P, and Ca fertiliser-additives. As shown in Fig. 3, when the HTC temperature and residence time increased, the Fe, P, K, Ca, Mg, Al, Mn, Na, and B contents of the hydrochar rose slightly but not as significant as in the case of biochar. This phenomenon can be attributed to the solubilisation of certain trace elements from microalgae biomass in the supercritical water environment, and their subsequent transfer into the liquid phase. The percentage of trace element loss appears to be comparable to the percentage of total solid weight loss. Combing proximate analysis and ICP-MS results, the biochar had a higher ash content and the hydrochar had a higher content of organic matter such as ketones, aldehydes, and carboxylic acids. In addition to the material characterisation, it is crucial to conduct lab-scale testing to examine the phytotoxicity of synthesised algal biochar and hydrochar, as these are proposed to be used as soil ameliorants and carbon storage agents.

3.3. Germination and seedling growth of raw biochar and hydrochar

In comparison to sand-only controls, the germination of *Nasturtium officinale* seeds was generally enhanced by biochars ranging from 1.1% to 11.0%, while it was significantly impeded by hydrochars ranging from 20.0% to 324.0%. As per the data shown in Fig. 4, MAB-550–20 had the most positive effect, while MAH-210–4 had the greatest negative impact.

Several previous studies have stated that the inhibition of germination can be attributed to the high/low pH (Kendrick and Drost, 2008; Mumme et al., 2018) and osmotic potential/salinity (Nhan et al., 2019). Potassium concentration is likely an important factor for low germination rate of seeds (Buss et al., 2016; Mumme et al., 2018; Ruttanaruangboworn et al., 2017). According to a study by Buss et al. (2016), excess potassium was found to indirectly hinder plant growth by elevating the pH levels in the solution. Biochar was observed to contain an active concentration of K^+ ions ranging from 154 to 231 mmol/L. The study concluded that the most probable mechanism for growth inhibition caused by excess potassium is an increase in osmotic pressure. A similar conclusion was made by Sosa et al. (2005), showing that K^+ was inhibitory on germination of *Prosopis strombulifera* seeds irrespective of the surrounding anion, and its inhibitory effect even stronger than that of Na^+. However, in this study, biochars with a high K content of 15304–26702 mg kg^{-1} did not show phytotoxicity but promotion effect, whereas hydrochars with relatively low K content (1699–2430 mg kg^{-1}) showed inhibition effect. Therefore, K concentration was not regarded as the dominant toxic effect in this case.

As shown in Fig. 4 the seed germination rate tended to decrease with HTC temperature increasing from 180 °C to 210 °C, and MAH-210–4 reached the highest phytotoxicity. Table 2 shows that higher HTC temperature and residence time can increase the pH of microalgae hydrochar. This is consistent with the content of potentially toxic substances, mainly carboxylic acids, identified by py-GC/MS total ion chromatography (Benavente et al., 2022). The presence of fatty acids containing aliphatic chains in microalgae hydrochar may contribute to this, as they are resistant to decomposition into smaller molecules during HTC at lower temperatures (Sun et al., 2021). As a result, remaining fatty acids can react with water to generate –COOH groups, leading to the formation of secondary char on the solid surface and a decrease in

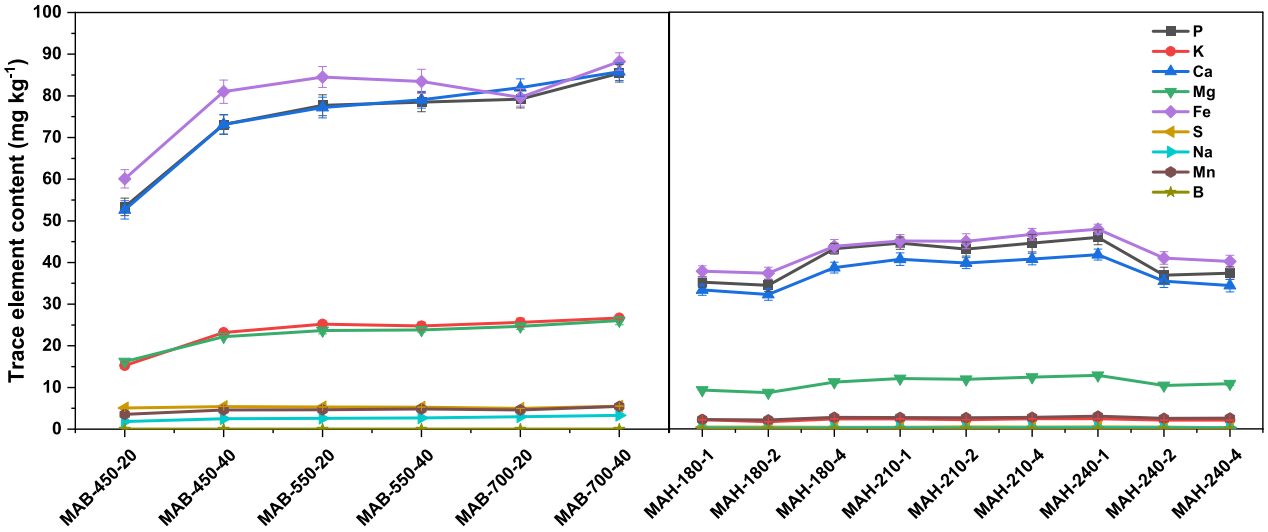

Fig. 3. Trace element contents in raw microalgae biochar and raw microalgae hydrochar.

Table 2
pH and electrical conductivity (EC) of raw biochar and hydrochar.

Samples	pH	Electrical conductivity (μS cm^{-1})
MAB-450–20	8.12	1780.0
MAB-450–40	8.22	1880.8
MAB-550–20	9.21	2389.5
MAB-550–40	9.32	3333.3
MAB-700–20	9.68	3250.2
MAB-700–40	9.88	3501.2
MAH-180–1	4.11	148
MAH-180–2	4.31	108
MAH-180–4	4.81	166
MAH-210–1	4.49	139
MAH-210–2	4.92	106
MAH-210–4	5.51	96.8
MAH-240–1	4.69	57.4
MAH-240–2	4.60	68.7
MAH-240–4	4.57	26.3

pH (Ischia et al., 2022). This phenomenon distinguishes microalgae hydrochar from lignocellulosic hydrochar, and highlights the importance of considering lipid composition in the production of hydrochar. Above 210 °C, the higher HTC temperature (240 °C) appears to have reduced the phytotoxicity of microalgae hydrochar, most likely by promoting decarboxylation reactions.

The seedling growth tests (Fig. 4) showed that, compared to the controlled blank group, average shoot and root lengths increased in the presence of biochar by around 17.2–51.3% and 11.1–52.2%, respectively, while decreased in presence of hydrochars by around 28.3–70.5% and 19.5–66.7%, respectively. Similar to the germination results, the tests with biochars showed a significant increase in both shoot and root lengths, however, its promotion effect did not show the same negative relationship with pyrolysis temperature (frm 450 to 700 °C) as the germination rate results. The reason for this might be that the interactions of soil moisture, nutrient adsorption, pyrolysis temperature, and residence time were very complex, hence, in-depth assessment of biochar physical properties and soil bioavailability should be explored in future tests. In this practical study, MAB-550–20 showed the highest shoot length (39.3 mm) and second highest shoot-to-root ratio (4.2); MAB-700–40 showed the highest root length (12.9 mm); MAB-700–20 showed the highest shoot-to-root ratio (4.6). Inorganic nutrients, especially Fe, P, and Ca, can be the major contributor to this phenomenon (Chew et al., 2022; Ng et al., 2022). As the contents of Fe, P, and Ca in the microalgae biochars increased with pyrolysis temperature, it is likely that this contributed to the enhanced shoot and root lengths. Results by Chew et al. (2022) also support the finding. The study showed that iron-rich biochar can upregulate root nitrate transporters, promote nitrogen absorption, and enhanced nutrient element uptake and growth in rice seedlings, resulting in increased shoot/root length of rice seedlings by about 33%. On the other hand, Ng et al. (2022) stated that P-rich biochar can provide available-P during seedling growth and promote formation polysaccharides and saponins. Comparatively, microalgae hydrochars still inhibited the growth of shoots and roots, due to the presence of phytotoxic compounds.

Some studies suggested that the seed germination rate can be improved by destructing the phytotoxic compounds of hydrochar using physical (Busch et al., 2013), chemical (Bahcivanji et al., 2020), and biological treatments (Busch et al., 2013). The phytotoxics compounds in hydrochars are likely to be solvent-soluble and volatile, and therefore this study chose two post-treatments aiming to mitigate the phytotoxicity of as-synthesised microalgae hydrochar in the following sections.

3.4. Impact of post-treatments (DCM washing and further pyrolysis) on hydrochar and its phytotoxicity

Since organic acids represented the main source of phytotoxic compounds, this study used DCM as a volatile and polar solvent to extract them as well as other VM from microalgae hydrochar, e.g., aldehydes, ketones, benzene, etc. (Benavente et al., 2022). With DCM washing, the VM content of hydrochar decreased by 0.5–38.9%. The highest VM variation was observed for the most severe HTC conditions (MAHW-240), indicating that high-temperature hydrochars were richer in extractable organic compounds as reported in Benavente et al. (2022), which was also in agreement with the germination results in Section 3.3. However, 51.4–57.6% of VM still remained in WAHW-240, while 33.1–41.49%, 41.4–46.4% remained in MAHW-180 and −210, respectively (see supplementary material). This implies that HTC with higher temperature transfer more extractable VM into non-extractable VM. However, the non-extractable contents of hydrochar have no significant impacts on the seed germination performance as shown in (see supplementary material). In addition, with the DCM washing treatment, ash contents of MAHW significantly increased by 4.3–85.1%. The reason for this would be that post-treatment with DCM was intended to separate the extractable fraction, especially VM, which included secondary char and fatty acids. However, ash contents cannot be dissolved in DCM solution, resulting in lower total solid yield accompanied with higher ash percentage. On the other hand, C and H daf% decreased dramatically, while the N, S, and O contents remained stable (see supplementary material), also mainly due to the removal of organic matters from the

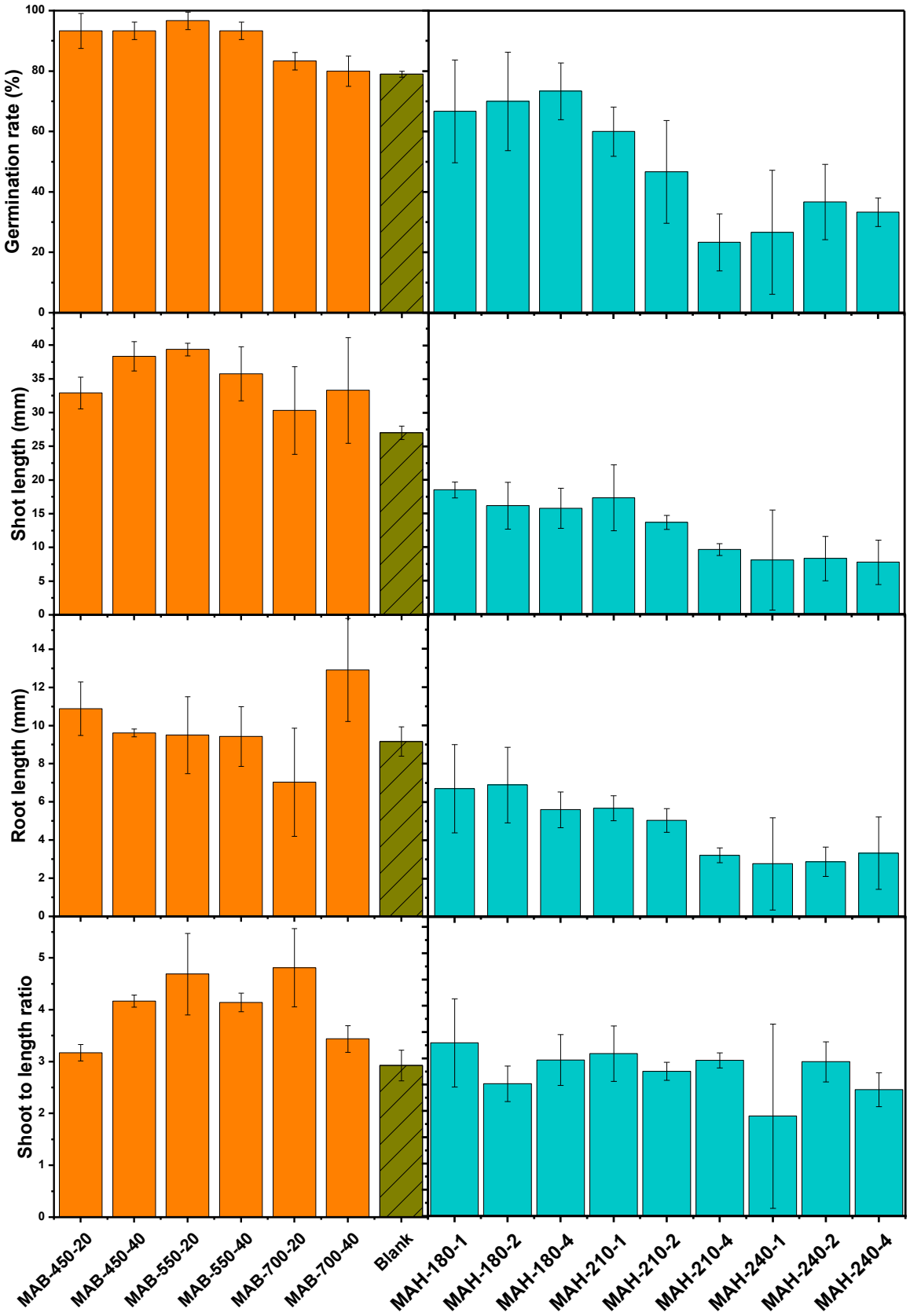

Fig. 4. Germination rate, shoot length, root length, and shoot-to-root ratio of raw biochar and hydrochar.

MAH.

DCM washing significantly improved the germination rates compared to that of MAH and even the blank controls. Especially, the highest promotion effect was shown in high-temperature MAHW, which indicated that phytotoxic organic compounds were effectively eliminated by DCM. This also provides indirect evidence that the toxic components are mainly present in the extractable fraction. The shoot and root lengths of DCM washed hydrochar were considered as expected results contributed by high ash/nutrient contents. The shoot and root lengths were enhanced by 52.9–242.0% and 15.7–148.2%, respectively (see supplementary material). The germination results implied that the interaction of nutrient content, ash content, extractable organic compound, and the resulting germination rate was complex. In short, DCM washing can substantially reduce the phytotoxic substances corresponding to organic compounds, and the promotion effect of microalgae hydrochar with high ash content as a soil amendment on seed germination needs to be further investigated. Importantly, the high ash/nutrient content of microalgae hydrochar can boost the shoot and root growth, but this promotion effect can be severely inhibited by the presence of organic compounds such as carboxylic acids, aldehydes, ketones phenolics, and benzene.

As discussed in previous sections, there is strong evidence that the phytotoxic substances contained in hydrochar were volatile organic compounds. Therefore, this study used pyrolysis as another post-treatment method to further treat MAH for reducing their toxicity. The pyrolysis condition was set to 550 °C, 25 °C/min heating rate, and 20 min residence time, since the MAB-550–20 showed the highest germination rate and shoot length, as well as relatively high root length. From the initial biomass, the total mass yield of MAHP varied from 20.7 to 24.9%. The solid yields of all MAHP remained almost consistent, unlike the yield performance of MAHW (Fig. 5). The further pyrolysis of hydrochar resulted in further devolatilisation and transfer of higher boiling point volatiles into liquid and gaseous products, further mitigating the phytotoxicity although not dramatically (see supplementary material). Generally, phytotoxicity was reduced in all MAHP (as compared to the control group), and seed germination performed best when grown in MAHP-210 environment (germination rate of 83.3–86.6%, shoot length of 31.0–32.6 mm, shot length of 7.0–9.6 mm, and shoot to length ratio of 3.2–4.9). It was observed that when applying pyrolysis as a post-treatment, the temperature and residence time in the initial HTC stage had minimal impact on the seed germination rate, and a high pyrolytic temperature of 550 °C effectively eliminated toxic substances present in the HTC char.

The MAHP exhibited a greater germination rate and shoot/root length than the MAHW, but shoot and root lengths were not substantially different and both were lower than in case of MAB, likely owing to the nutrient loss. Nutrients were transferred into the liquid phase during HTC stage, with only a small further loss in the DCM wash and further pyrolysis.

3.5. Carbon sequestration potential

The results clearly showed that MAHP is effective in enhancing seed germination and providing nutrients for seedling growth. However, it was found that it can only sequester 2/3 as much carbon as MAB due to primary C loss during the HTC process (as shown in Fig. 6). While biochar has the potential to mitigate climate change by sequestering carbon in the soil for several hundred to thousands of years, the use of hydrochar as a soil amendment may increase CO_2 and CH_4 emissions (Zhou et al., 2018). Therefore, it is crucial to perform carbon balance calculations for microalgae biochar and hydrochar. In terms of carbon sequestration, MAB performed better than MAHP, retaining 31.8–34.7% of carbon from the raw microalgae biomass compared to 20.3–25.5% in case of MAHP. On the other hand, while both MAH (up to 58.8%) and MAHW (up to 47.8%) retained more carbon than MAB (up to 34.7%), this consisted mainly of unstable carbon due to the low temperature in

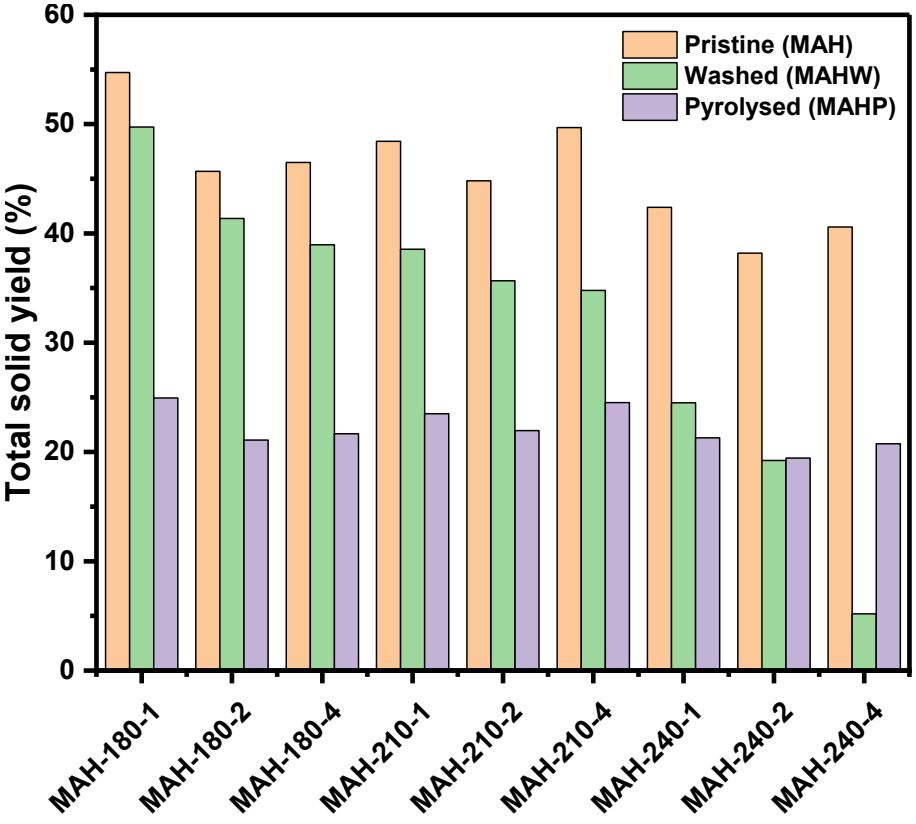

Fig. 5. Total solid yields of raw hydrochar and hydrochar with two post-treatments.

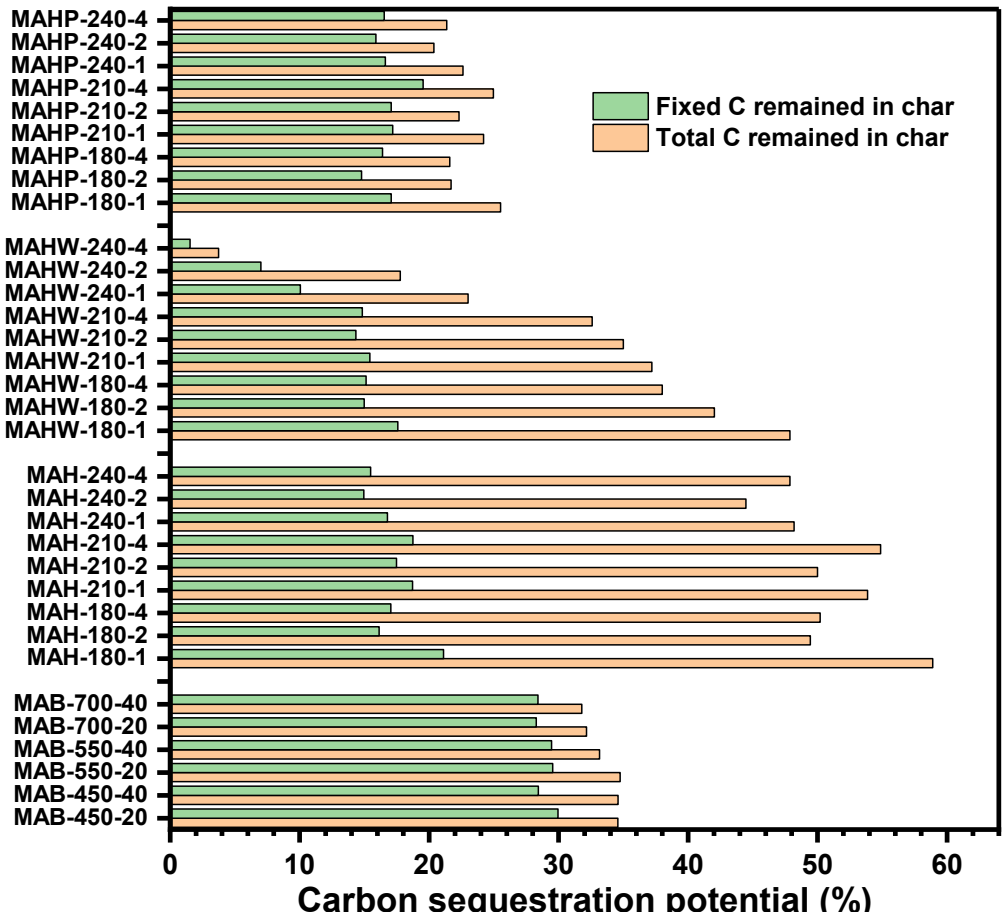

Fig. 6. Carbon sequestration potential of microalgae biochar and hydrochar.

the HTC process. Only 15.6–17.3% and 13.0–18.8% fixed carbon were presented in MAH and MAHW, respectively, compared to 35.8–38.6% fixed carbon found in MAB (Table 1; Fig. 6; see supplementary material). Long-term pot testing for the carbon stability comparison of microalgae biochar and hydrochar were suggested because this study only conducted 7-day germination and seedling growth tests.

DCM washing and further pyrolysis are effective post-treatment methods for producing hydrochar suitable for use as a soil amendment. However, they have several drawbacks such as lower carbon sequestration rates and higher operational costs.

4. Conclusion

The results of study comparing microalgae biochar and hydrochar for soil application indicated that while biochar can be used directly, hydrochar requires post-treatment to reduce phytotoxic compounds. Chemical or thermal processes effectively reduce these compounds, as demonstrated by DCM washing and pyrolysis. This mitigates the phytotoxicity of hydrochar and highlights the potential of HTC for producing microalgae-based hydrochar with minimal environmental impact. However, further comprehensive assessment is necessary to understand its complete life cycle impact and carbon storage potential. Additionally, the high nitrogen content of algae-based biochar suggests potential benefits in other applications, which require further investigation.

CRediT authorship contribution statement

Jiacheng Sun: Conceptualization, Investigation, Writing – original draft. **Veronica Benavente:** Investigation, Writing – review & editing. **Stina Jansson:** Supervision, Writing – review & editing. **Ondřej Mašek:** Supervision, Writing – review & editing.

Declaration of Competing Interest

The authors declare that they have no known competing financial interests or personal relationships that could have appeared to influence the work reported in this paper.

Data availability

Data will be made available on request.

Acknowledgments

J. Sun acknowledges Scottish Alliance for Geoscience, Environment, and Society (SAGES) for supporting this work.

Appendix A. Supplementary data

Supplementary data to this article can be found online at https://doi.org/10.1016/j.biortech.2023.129567.

References

Abdel-Raouf, N., Al-Homaidan, A.A., Ibraheem, I.B.M., 2012. Microalgae and wastewater treatment. Saudi J. Biol. Sci. 19, 257–275. https://doi.org/10.1016/j.sjbs.2012.04.005.

Bahcivanji, L., Gascó, G., Paz-Ferreiro, J., Méndez, A., 2020. The effect of post-pyrolysis treatment on waste biomass derived hydrochar. Waste Manag. 106, 55–61. https://doi.org/10.1016/j.wasman.2020.03.007.

Bakshi, S., Banik, C., Laird, D.A., 2020. Estimating the organic oxygen content of biochar. Sci. Rep. 10, 1–12. https://doi.org/10.1038/s41598-020-69798-y.
Benavente, V., Lage, S., Gentili, F.G., Jansson, S., 2022. Influence of lipid extraction and processing conditions on hydrothermal conversion of microalgae feedstocks – Effect on hydrochar composition, secondary char formation and phytotoxicity. Chem. Eng. J. 428, 129559 https://doi.org/10.1016/j.cej.2021.129559.
Bevan, E., Fu, J., Zheng, Y., 2020. Challenges and opportunities of hydrothermal carbonisation in the UK; Case study in Chirnside. RSC Adv. 10, 31586–31610. https://doi.org/10.1039/d0ra04607h.
Binda, G., Spanu, D., Bettinetti, R., Magagnin, L., Pozzi, A., Dossi, C., 2020. Comprehensive comparison of microalgae-derived biochar from different feedstocks: A prospective study for future environmental applications. Algal Res. 52, 102103 https://doi.org/10.1016/j.algal.2020.102103.
Busch, D., Stark, A., Kammann, C.I., Glaser, B., 2013. Genotoxic and phytotoxic risk assessment of fresh and treated hydrochar from hydrothermal carbonization compared to biochar from pyrolysis. Ecotoxicol. Environ. Saf. 97, 59–66. https://doi.org/10.1016/j.ecoenv.2013.07.003.
Buss, W., Graham, M.C., Shepherd, J.G., Mašek, O., 2016. Risks and benefits of marginal biomass-derived biochars for plant growth. Sci. Total Environ. 569–570, 496–506. https://doi.org/10.1016/j.scitotenv.2016.06.129.
Buss, W., Jansson, S., Wurzer, C., Mašek, O., 2019. Synergies between BECCS and Biochar - Maximizing Carbon Sequestration Potential by Recycling Wood Ash. ACS Sustain. Chem. Eng. 7, 4204–4209. https://doi.org/10.1021/acssuschemeng.8b05871.
Buss, W., Hertzog, J., Pietrzyk, J., Carré, V., Mackay, C.L., Aubriet, F., Mašek, O., 2021. Comparison of pyrolysis liquids from continuous and batch biochar production—influence of feedstock evidenced by fticr ms. Energies 14 (1), 9.
Castro, J.d.S., Assemany, P.P., Carneiro, A.C.d.O., Ferreira, J., de Jesus Júnior, M.M., Rodrigues, F.d.Á., Calijuri, M.L., 2021. Hydrothermal carbonization of microalgae biomass produced in agro-industrial effluent: Products, characterization and applications. Sci. Total Environ. 768, 144480.
Chew, J.K., Joseph, S., Chen, G., Zhang, Y., Zhu, L., Liu, M., Taherymoosavi, S., Munroe, P., Mitchell, D.R.G., Pan, G., Li, L., Bian, R., Fan, X., 2022. Biochar-based fertiliser enhances nutrient uptake and transport in rice seedlings. Sci. Total Environ. 826, 154174 https://doi.org/10.1016/J.SCITOTENV.2022.154174.
Chu, Q., Xue, L., Cheng, Y., Liu, Y., Feng, Y., Yu, S., Meng, L., Pan, G., Hou, P., Duan, J., Yang, L., 2020. Microalgae-derived hydrochar application on rice paddy soil: Higher rice yield but increased gaseous nitrogen loss. Sci. Total Environ. 717, 137127 https://doi.org/10.1016/j.scitotenv.2020.137127.
Cong, H., Mašek, O., Zhao, L., Yao, Z., Meng, H., Hu, E., Ma, T., 2018. Slow Pyrolysis Performance and Energy Balance of Corn Stover in Continuous Pyrolysis-Based Poly-Generation Systems. Energy and Fuels 32 (3), 3743–3750.
de Jager, M., Giani, L., 2021. An investigation of the effects of hydrochar application rate on soil amelioration and plant growth in three diverse soils. Biochar 3, 349–365. https://doi.org/10.1007/s42773-021-00089-z.
Ding, Z., Zhang, L., Mo, H., Chen, Y., Hu, X., 2021. Microwave-assisted catalytic hydrothermal carbonization of Laminaria japonica for hydrochars catalyzed and activated by potassium compounds. Bioresour. Technol. 341, 125835.
European Biochar Foundation (EBC), 2016. Guidelines for a Sustainable Production of Biochar. Eur. Biochar Found, pp. 1–22.
Fu, X., Li, Q., Hu, C., 2019. Identification and structural characterization of oligomers formed from the pyrolysis of biomass. J. Anal. Appl. Pyrolysis 144, 104696. https://doi.org/10.1016/j.jaap.2019.104696.
Gai, C., Zhang, Y., Chen, W.T., Zhang, P., Dong, Y., 2013. Thermogravimetric and kinetic analysis of thermal decomposition characteristics of low-lipid microalgae. Bioresour. Technol. 150, 139–148. https://doi.org/10.1016/j.biortech.2013.09.137.
Gautam, R., Varma, A.K., Vinu, R., 2017. Apparent kinetics of fast pyrolysis of four different microalgae and product analyses using pyrolysis-FTIR and pyrolysis-GC/MS. Energy and Fuels 31 (11), 12339–12349.
Ho, S.-H., Huang, S.-W., Chen, C.-Y., Hasunuma, T., Kondo, A., Chang, J.-S., 2013. Characterization and optimization of carbohydrate production from an indigenous microalga Chlorella vulgaris FSP-E. Bioresour. Technol. 135, 157–165.
IBI, I.B.I., 2015. Standardized product definition and product testing guidelines for biochar that is used in soil. Int. Biochar Initiat. 23.
Ischia, G., Cutillo, M., Guella, G., Bazzanella, N., Cazzanelli, M., Orlandi, M., Miotello, A., Fiori, L., 2022. Hydrothermal carbonization of glucose: Secondary char properties, reaction pathways, and kinetics. Chem. Eng. J. 449, 137827 https://doi.org/10.1016/J.CEJ.2022.137827.
Kambo, H.S., Dutta, A., 2015. A comparative review of biochar and hydrochar in terms of production, physico-chemical properties and applications. Renew. Sustain. Energy Rev. 45, 359–378. https://doi.org/10.1016/j.rser.2015.01.050.
Kendrick, T., Drost, D., 2008. Watercress in the Garden.
Khan, T.A., Saud, A.S., Jamari, S.S., Rahim, M.H.A., Park, J.W., Kim, H.J., 2019. Hydrothermal carbonization of lignocellulosic biomass for carbon rich material preparation: A review. Biomass Bioenergy 130, 105384. https://doi.org/10.1016/j.biombioe.2019.105384.
Lee, J., Lee, K., Sohn, D., Kim, Y.M., Park, K.Y., 2018. Hydrothermal carbonization of lipid extracted algae for hydrochar production and feasibility of using hydrochar as a solid fuel. Energy 153, 913–920. https://doi.org/10.1016/j.energy.2018.04.112.
Li, S., Show, P.L., Ngo, H.H., Ho, S.-H., 2022. Algae-mediated antibiotic wastewater treatment: A critical review. Environ. Sci. Ecotechnology 9, 100145. https://doi.org/10.1016/j.ese.2022.100145.
Lucian, M., Volpe, M., Gao, L., Piro, G., Goldfarb, J.L., Fiori, L., 2018. Impact of hydrothermal carbonization conditions on the formation of hydrochars and secondary chars from the organic fraction of municipal solid waste. Fuel 233, 257–268. https://doi.org/10.1016/j.fuel.2018.06.060.
Magida, N.E., Bolo, L.L., Hlangothi, S.P., Dugmore, G., Ogunlaja, A.S., 2021. Co-combustion Characteristics of coal-Scenedesmus Microalgae Blends and Their Resulting Ash. Combust. Sci. Technol. 193, 419–436. https://doi.org/10.1080/00102202.2019.1658577.
Mašek, O., Buss, W., Roy-Poirier, A., Lowe, W., Peters, C., Brownsort, P., Mignard, D., Pritchard, C., Sohi, S., 2018. Consistency of biochar properties over time and production scales: A characterisation of standard materials. J. Anal. Appl. Pyrolysis 132, 200–210. https://doi.org/10.1016/j.jaap.2018.02.020.
Mašek, O., Buss, W., Brownsort, P., Rovere, M., Tagliaferro, A., Zhao, L., Cao, X., Xu, G., 2019. Potassium doping increases biochar carbon sequestration potential by 45%, facilitating decoupling of carbon sequestration from soil improvement. Sci. Rep. 9, 1–8. https://doi.org/10.1038/s41598-019-41953-0.
Michalak, I., Baśladyńska, S., Mokrzycki, J., Rutkowski, P., 2019. Biochar from a freshwater macroalga as a potential biosorbent for wastewater treatment. Water (Switzerland) 11, 4–6. https://doi.org/10.3390/w11071390.
Mohsenpour, S.F., Hennige, S., Willoughby, N., Adeloye, A., Gutierrez, T., 2021. Integrating micro-algae into wastewater treatment: A review. Sci. Total Environ. 752, 142168 https://doi.org/10.1016/j.scitotenv.2020.142168.
Mumme, J., Getz, J., Prasad, M., Lüder, U., Kern, J., Mašek, O., Buss, W., 2018. Toxicity screening of biochar-mineral composites using germination tests. Chemosphere 207, 91–100. https://doi.org/10.1016/j.chemosphere.2018.05.042.
Ng, C.W.W., Wang, Y.C., Ni, J.J., So, P.S., 2022. Effects of phosphorus-modified biochar as a soil amendment on the growth and quality of Pseudostellaria heterophylla. Sci. Rep. 12 https://doi.org/10.1038/s41598-022-11170-3.
Nhan, H.T., Tai, N.T., Liem, P.T., Ut, V.N., Ako, H., 2019. Effects of different stocking densities on growth performance of Asian swamp eel Monopterus albus, water quality and plant growth of watercress Nasturtium officinale in an aquaponic recirculating system. Aquaculture 503, 96–104. https://doi.org/10.1016/j.aquaculture.2018.12.067.
Ruttanaruangboworn, A., Chanprasert, W., Tobunluepop, P., Onwimol, D., 2017. Effect of seed priming with different concentrations of potassium nitrate on the pattern of seed imbibition and germination of rice (Oryza sativa L.). J. Integr. Agric. 16, 605–613. https://doi.org/10.1016/S2095-3119(16)61441-7.
Shyam, S., Arun, J., Gopinath, K.P., Ribhu, G., Ashish, M., Ajay, S., 2022. Biomass as source for hydrochar and biochar production to recover phosphates from wastewater: A review on challenges, commercialization, and future perspectives. Chemosphere 286, 131490. https://doi.org/10.1016/j.chemosphere.2021.131490.
Sosa, L., Llanes, A., Reinoso, H., Reginato, M., Luna, V., 2005. Osmotic and specific ion effects on the germination of Prosopis strombulifera. Ann. Bot. 96, 261–267. https://doi.org/10.1093/aob/mci173.
Sun, J., Norouzi, O., Mašek, O., 2021. A state-of-the-art review on algae pyrolysis for bioenergy and biochar production. Bioresour. Technol. 346, 126258.
Wang, K., Brown, R.C., 2013. Catalytic pyrolysis of microalgae for production of aromatics and ammonia. Green Chem. 15 (3), 675.
Wurzer, C., Mašek, O., 2021. Feedstock doping using iron rich waste increases the pyrolysis gas yield and adsorption performance of magnetic biochar for emerging contaminants. Bioresour. Technol. 321, 124473.
Yin, X., Peñuelas, J., Sardans, J., Xu, X., Chen, Y., Fang, Y., Wu, L., Singh, B.P., Tavakkoli, E., Wang, W., 2021. Effects of nitrogen-enriched biochar on rice growth and yield, iron dynamics, and soil carbon storage and emissions: A tool to improve sustainable rice cultivation. Environ. Pollut. 287, 117565.
Zhang, J., Huang, D., Shao, J., Zhang, X., Zhang, S., Yang, H., Chen, H., 2022. A new nitrogen-enriched biochar modified by ZIF-8 grafting and annealing for enhancing CO2 adsorption. Fuel Process. Technol. 231, 107250 https://doi.org/10.1016/j.fuproc.2022.107250.
Zhang, L., Liu, S., Wang, B., Wang, Q., Yang, G., Chen, J., 2015. Effect of residence time on hydrothermal carbonization of corn cob residual. BioResources 10, 3979–3986. https://doi.org/10.15376/biores.10.3.3979-3986.
Zheng, H., Guo, W., Li, S., Chen, Y., Wu, Q., Feng, X., Yin, R., Ho, S.H., Ren, N., Chang, J. S., 2017. Adsorption of p-nitrophenols (PNP) on microalgal biochar: Analysis of high adsorption capacity and mechanism. Bioresour. Technol. 244, 1456–1464. https://doi.org/10.1016/j.biortech.2017.05.025.
Zhou, B., Feng, Y., Wang, Y., Yang, L., Xue, L., Xing, B., 2018. Impact of hydrochar on rice paddy CH4 and N2O emissions: A comparative study with pyrochar. Chemosphere 204, 474–482. https://doi.org/10.1016/j.chemosphere.2018.04.056.